Journal of Alloys and Compounds 503 (2010) 122–126

Contents lists available at ScienceDirect

Journal of Alloys and Compounds

journal homepage: www.elsevier.com/locate/jallcom

Production and corrosion behaviours of the Al–12Si–*X*Mg alloys containing in situ Mg_2Si particles

H. Ahlatci*

Karabuk University, Engineering Faculty, Department of Metallurgy and Materials, 78050/Karabuk, Turkey

ARTICLE INFO

Article history:
Received 8 January 2010
Received in revised form 21 April 2010
Accepted 28 April 2010
Available online 5 May 2010

Keywords:
Al–Si alloy
Corrosion properties
Mg
In situ Mg_2Si particles

ABSTRACT

In this study the mechanical behaviours of Al–12Si–*X*Mg alloys (where Mg contents varied up to 20%) have been investigated. The alloys were prepared by casting followed by extrusion at 300 °C with a ratio of 1.6. Precipitation of the Mg_2Si phases was observed in the Mg containing Al–12Si alloys as two different morphologies; i.e., as a polyhedral primary particle and as a Chinese script. Results showed that volume fraction and size of the primary Mg_2Si particles increased with increasing the Mg content. Mg containing alloys exhibited higher hardness, compression strength and lower corrosion resistance than the Mg free alloy.

1. Introduction

Among the materials of the tribological importance, hypereutectic Al–Si alloys preferentially have received considerable attention for wear related applications such as internal combustion engines, pistons, liners, pulleys, rockers and pivots. Reduction in density and thermal expansion coefficient, improvement in hardness, ambient temperature mechanical properties (modulus and strength) and wear resistance along with an excellent castability can be achieved by addition of Si to Al. However, increase in Si content gives rise to coarsening of eutectic Si, encouraging formation of relatively brittle needle Si phase in the microstructure, which leads to deterioration of mechanical properties of the alloy [1–3].

An alternative approach to the production of Al–Si alloys with improved mechanical properties is to reinforce the matrix with hard ceramic particles, such as SiC and Al_2O_3 [4,5]. It should be mentioned that most of the metal matrix composites suffer from thermodynamic instability of interfaces among the ceramic reinforcement/matrix and poor wettability of the reinforcement [6]. Additionally, small particle size of the reinforcement and the density differences between the reinforcement and the matrix make the fabrication of the composites more difficult [7]. Recently, a new in situ particle reinforced alloys have been synthesized by nucleation and growth of the reinforcement from parent matrix as an alternative to conventional composites reinforced with external ceramic particles [8–24]. As compared to the conventional metal matrix composite fabrication, this new process has advantages of inherently stable and equilibrium interface between the reinforcement and matrix along with an easy production at low costs [8–24].

Since the intermetallic compound Mg_2Si exhibits low density, low thermal expansion coefficient, high melting temperature, high hardness and elastic modulus [9,13,15], it is an attractive candidate for in situ reinforcing of Mg and Al alloys. In previous studies [7–14,19,20] in situ Mg_2Si reinforced composites produced by ingot casting metallurgy did not display satisfying mechanical properties due to the large size and brittle dendritic solidification characteristics of both the Mg_2Si phase and matrix. Therefore, several researches have been correspondingly focused on the refinement and modification of Mg_2Si phases by addition of red phosphorous [8], Ca or P [12], rare earth elements [14], mischmetal of Ce–30La–17Nd–10Pr [14], sodium salts of NaCl–30$MgCl_2$–10KCl or NaCl–NaF–KCl [11,16], strontium [11,17,21,22], Ce [22] and mixture of K_2TiF_6 and KBF_4 [18,23] to the melt.

Considerable amount of researches are available in the literature [8–24], concerning the preparation and processing of the in situ alloys containing Mg_2Si particles as the reinforcement. However, reports on the corrosion behaviour of the in situ composites seem to be scarce. Therefore, this work deals with the mechanical and corrosion behaviours of the in situ Mg_2Si reinforced Al–12Si–*X*Mg alloys.

2. Materials and methods

Commercially pure 12 wt.% Si containing Al ingot alloy and pure Mg were used as starting materials to prepare the Al–12Si–*X*Mg alloys. The Mg contents varied between 0 wt.% and 20 wt.% in the investigated alloys. The Mg was added to the

* Tel.: +90 370 433 20 21; fax: +90 370 433 32 90.
E-mail address: hahlatci@karabuk.edu.tr.

0925-8388/$ – see front matter © 2010 Elsevier B.V. All rights reserved.
doi:10.1016/j.jallcom.2010.04.214

Table 1
The chemical composition (%) of the investigated alloys.

	Si	Mg	Fe	Cu	Mn	Zn	Ti	Al
Al–12Si–0Mg	13.5	0.1	0.6	0.1	0.4	0.1	0.15	85.1
Al–12Si–5Mg	11.3	5.2	1.5	0.2	0.3	0.1	0.05	81.7
Al–12Si–10Mg	11.1	11.0	1.7	0.2	0.2	0.1	0.05	76.7
Al–12Si–20Mg	12.2	19.1	2.1	0.3	0.3	0.1	0.05	65.9

Al–12Si alloy melt at 800 °C along with 0.05% of Sr, 0.20% of red phosphorous and 0.30% of NaCl + 30$MgCl_2$ + 10KCl mixtures which were all preheated at 300 °C before charging into the melt. In order to balance the oxidation loss the above additions were charged with an extra of 15 wt.%. Degassing was conducted by using C_6Cl_6 before casting. After cleaning the slag, the melt was poured at 800 °C into a chill mould to produce the rod shaped ingots of 20 mm in diameter and 300 mm in length. After casting, the rods were extruded directly to 16 mm diameter (corresponding to extrusion ratio of 1.6) at 300 °C. Chemical compositions of the investigated alloys determined by optic emission methods are given in Table 1.

Characterizations of the extruded rods were carried out by mechanical and corrosion tests as well as microstructural examinations.

Microstructural survey of the extruded Al–12Si–*X*Mg alloys was conducted on an optical light microscope (LOM) after preparing the samples according to standard metallographic procedures. Volume fractions and average sizes of the phases present in the microstructures of the investigated alloys were measured by using linear intercept method. For linear intercept methods 5 different photographs were taken from the surface of the each sample and then 10 lines were drawn on the each photograph. The phases were identified with Cu Kα on an X-ray diffractometer.

Room temperature mechanical properties of the alloys were determined by hardness measurements and compression tests. Hardness survey of the investigated alloys was measured on Shimadzu HMV2 microhardness tester by applying indentation load of 2000 g with a Vickers indenter. At least, ten successive measurements were made for each condition. Round specimens with 20 mm of length and 10 mm of diameter were tested by a Dartec Universal testing machine at a crosshead speed of 0.5 mm/min to determine the compression behaviour of the alloys. The results of the compression tests were compiled by averaging the decision of five specimens.

Corrosion tests were carried out on the basis of intergranular corrosion tests by considering ISO 11846 standards. The corrosion behaviour of the alloys was examined by immersing the samples in a solution of "30 g/l NaCl + 10 ml/l HCl" in deionized water in a Pyrex glass cell exposed to atmospheric air. The amount of the solution in the beaker was estimated by taking into account the surface area of the specimens as 0.3 ml/mm^2. Evaluation of the corrosion was determined by weight loss-measuring test and by potentiodynamic polarization measurement. After the tests the samples were cleaned in 50 vol% nitric acid for 3 min as recommended by ASTM G1-90 and were dried. At least three samples were subjected to immersion tests and average values of three samples are reported.

For the weight loss-measuring test the disc shaped samples (20 mm × 15 mm × 4 mm) were suspended in the solution with a plastic string for 12 h. Before immersing in the solution the surfaces of the samples were ground with 1200 mesh SiC abrasive paper and then cleaned with deionized water followed by rinsing with methanol and dried. After the test, the samples cleaned/dried were weighed by an electronic balance having a resolution of ±0.1 mg. The normalized weight loss values of the investigated alloys were calculated in the unit of g/mm^2 by dividing the weight loss of the each sample by their initial total surface area.

For the potentiodynamic polarization measurement, machined samples (10 mm in length and 15 mm diameter) were mounted on copper rod using epoxy resin for electrical connection, and open surface of all samples were polished with up to 1200 grit SiC emery paper and then cleaned with deionized water followed by rinsing with methanol and dried. The potentiodynamic polarization measurement was carried out at room temperature using a Gamry model PC4/300 mA potentiostat/galvanostat controlled by a computer with DC 105 Corrosion analysis software. The electrochemical cell consisted three electrodes: a working electrode, a reference electrode (a saturated calomel electrode, SCE) and a counter electrode (a carbon rod). During the electrochemical corrosion test, the electrode potential was scanned at a scan rate of 10 mV/min from −1000 mV towards anodic potential and the corrosion current values were recorded in 1 mV steps for both anodic and cathodic polarization in the unit of mA/cm^2 by dividing the current values of the each sample by their initial total surface area.

Finally, the surfaces of the samples were examined with a LOM. Cross-sections of the samples were also investigated by a LOM and scanning electron microscope (SEM) after employing conventional metallographic preparation procedure in order to examine corrosion penetration through the thickness.

3. Results and discussion

Microstructures of the extruded Al–12Si–*X*Mg alloys are shown in Fig. 1. The microstructures were mainly composed of needle

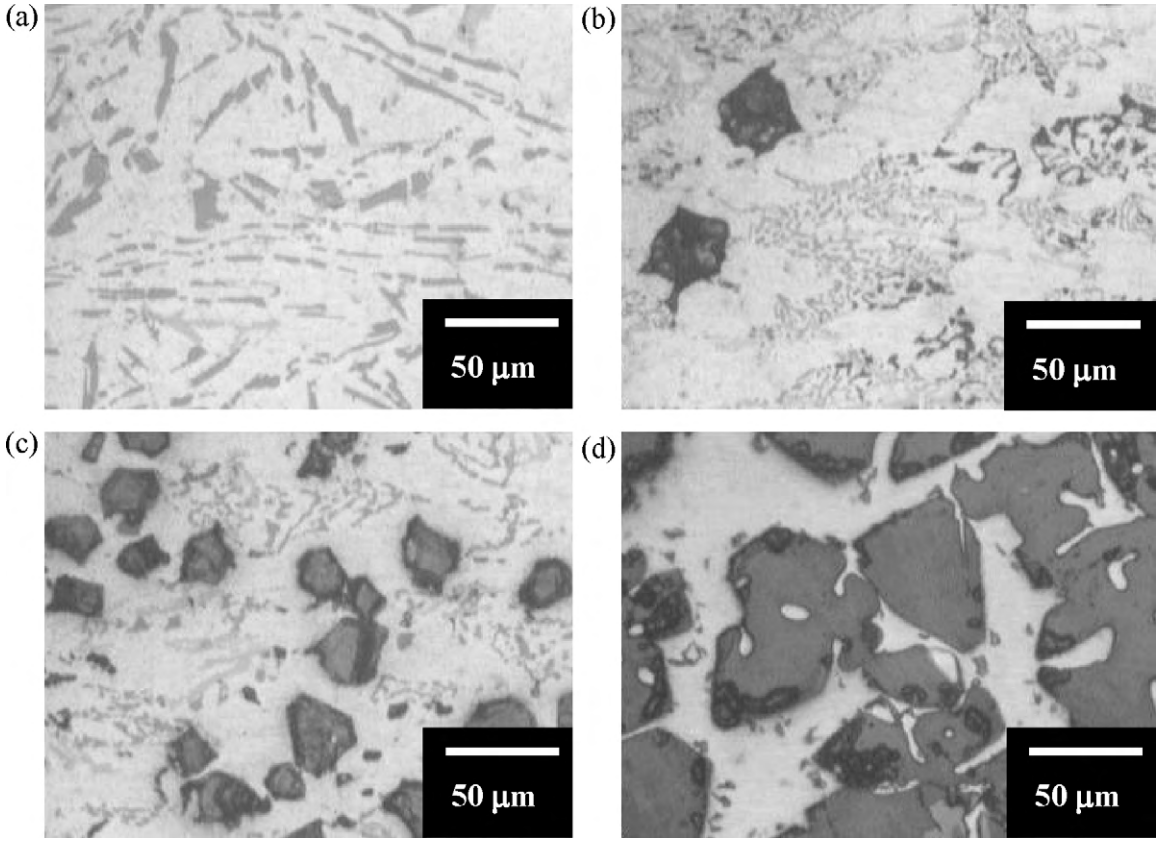

Fig. 1. LOM micrographs of the (a) Mg free, (b) 5 wt.% Mg, (c) 10 wt.% Mg and (d) 20 wt.% Mg containing alloys.

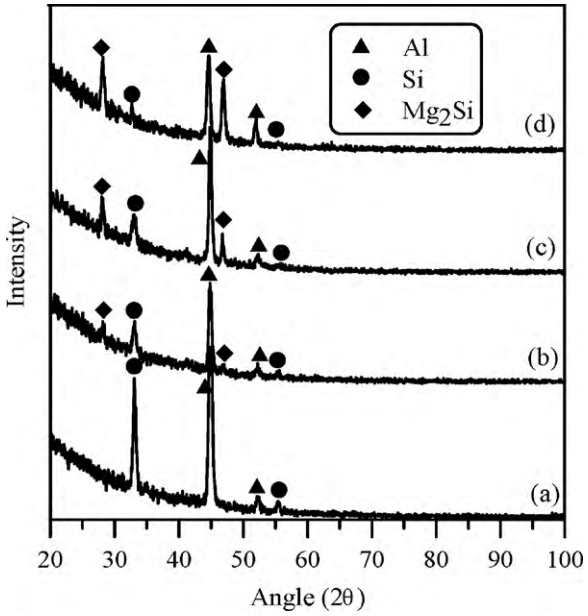

Fig. 2. XRD patterns of the (a) Mg free, (b) 5 wt.% Mg, (c) 10 wt.% Mg and (d) 20 wt.% Mg containing alloys.

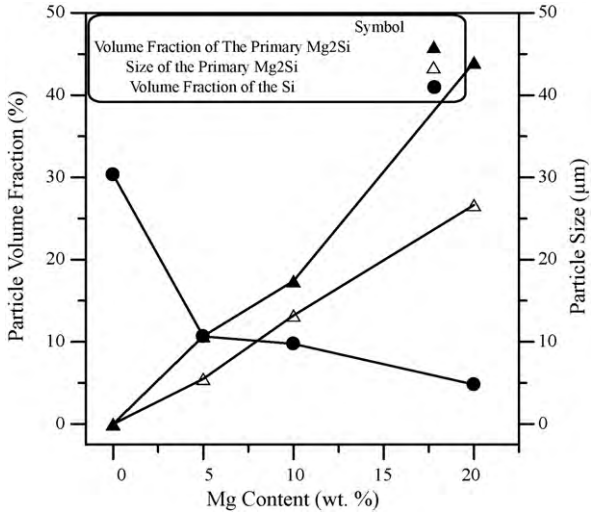

Fig. 3. The effect of Mg content of the alloys on size of the primary Mg_2Si particles, the volume fraction of the primary Mg_2Si and Si particles.

shaped light grey colored phases, polygonal shape dark particles, Chinese script and white colored matrix. Porosities were not detected in the microstructures. Considering the results of the XRD analysis presented in Fig. 2, the microstructural constituents were identified as Si (needle shaped light gray color phases), Mg_2Si and Al (white colored matrix). Mg_2Si appeared in two different morphologies (i.e., polyhedral shape dark particles and grey colored Chinese script phases) as mentioned in the literature [8–28].

Since the compositions of the investigated alloys were hypereutectic, it is suggested that the polyhedral dark particles, which were identified as primary Mg_2Si particles, were in situ formed during initial stage of the solidification process. Although the forming mechanism of the primary Mg_2Si particles has not been explained clearly, the addition of the modifiers such as Sr, red phosphorus and salt mixtures to the melt may result in an increase in the number of nuclei and changed in the morphology and size of the primary Mg_2Si particles [14,18,21–23] by suppressing their anisotropic growth through modifying both the solid-liquid interfacial energy and surface energy of the solid Mg_2Si phase or by poisoning the surface of the in situ Mg_2Si nuclei owing to the segregation of Na or K at the liquid–solid interface [7,10,11].

Detailed microstructural examinations revealed that the primary Mg_2Si particles were homogeneously distributed in the microstructures (Fig. 1). The variation of the size of the primary Mg_2Si particles, the volume fraction of the primary Mg_2Si and Si particles against the Mg contents is presented in Fig. 3. Upon increase of the Mg, the volume fraction and size of the primary Mg_2Si particles precipitated in the matrix increased linearly while the volume fraction of the Si needle particles decreased. The microscopic studies also revealed that, in the Al–12Si–20Mg alloy, the morphology of the primary Mg_2Si particles formed as irregular shape, whereas the Chinese script Mg_2Si phases were refined (Fig. 1). As seen in Table 1, to generate the primary and Chinese script Mg_2Si, almost all of the Si element reacted with Mg in the Al–12Si–20Mg alloy.

The results of the room temperature mechanical tests are plotted in Fig. 4, against the Mg content of the investigated alloys. The hardness and compression strength increased with increasing the Mg content of the alloy attributed to the increment of the primary Mg_2Si volume fraction and size. The addition of the 10 wt.% Mg

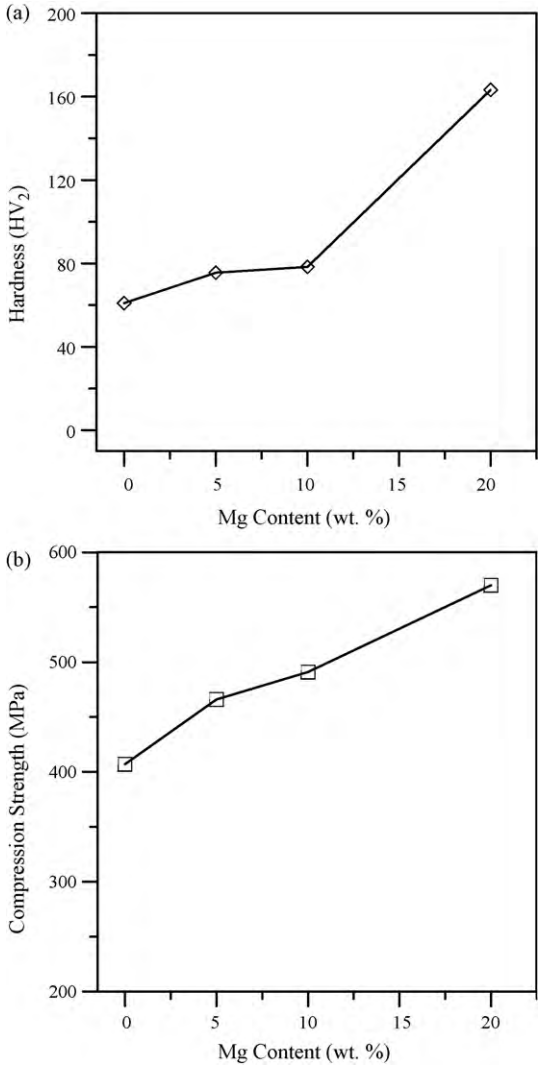

Fig. 4. The effect of Mg content on the (a) hardness and (b) compression strength of the investigated alloys.

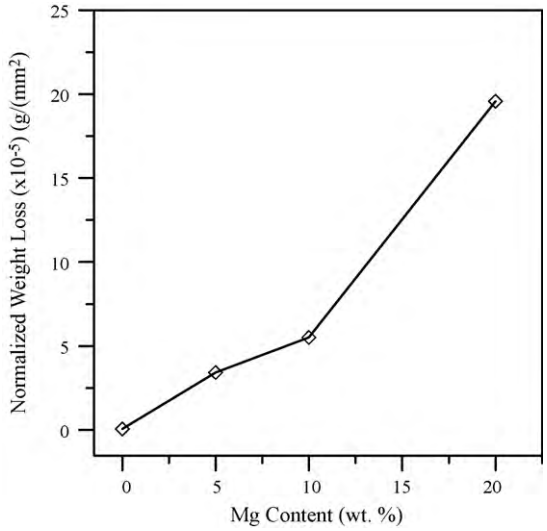

Fig. 5. The effect of the Mg content on the weight loss-measuring test of the investigated alloys.

yielded the hardness value of 80 HV_2, which is 30% higher than the hardness of the Mg free alloy. Further addition of the Mg resulted in severe hardening. The hardness of the Al–12Si–20Mg alloy was almost two fold of that of the Al–12Si–10Mg alloy. The increase in compression strength is continual with increasing the Mg content. The mechanism of hardening was believed to be due to the combination of solid solution and formation of the in situ particles being obstacles to the movement of dislocations [5,29].

The results of the weight loss-measuring test are presented in Fig. 5 as the variation of the normalized weight loss values with respect to the Mg content of the examined alloys. Higher corrosion loss was detected with increasing the Mg content of the alloys (especially above 10 wt.% Mg). The results of the potentiodynamic polarization measurement are shown in Fig. 6 according to Mg addition. The polarization results showed that the corrosion potential (E_{corr}) is relatively constant (Fig. 6a) while the corrosion current density (I_{corr}) of the Al–12Si alloy altered with varying Mg alloying addition. The variation in the I_{corr}, extracted from the polarization curves, as a function of the Mg content in the alloy is given in Fig. 6b. The polarization results are very much in line with the weight loss-measuring test results.

LOM micrographs of the surfaces and cross-sections of the corroded alloys are displayed in Fig. 7. Corrosion attack was localized

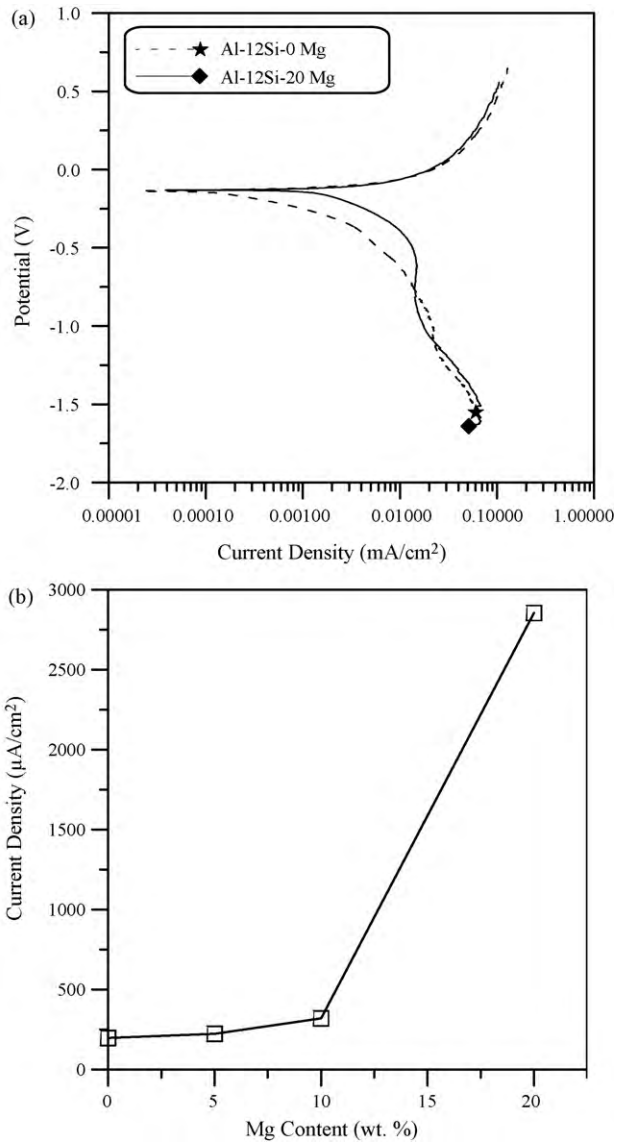

Fig. 6. The effect of the Mg content on the potentiodynamic polarization measurement: the (a) potentiodynamic polarization curve and (b) corrosion current density of the investigated alloys.

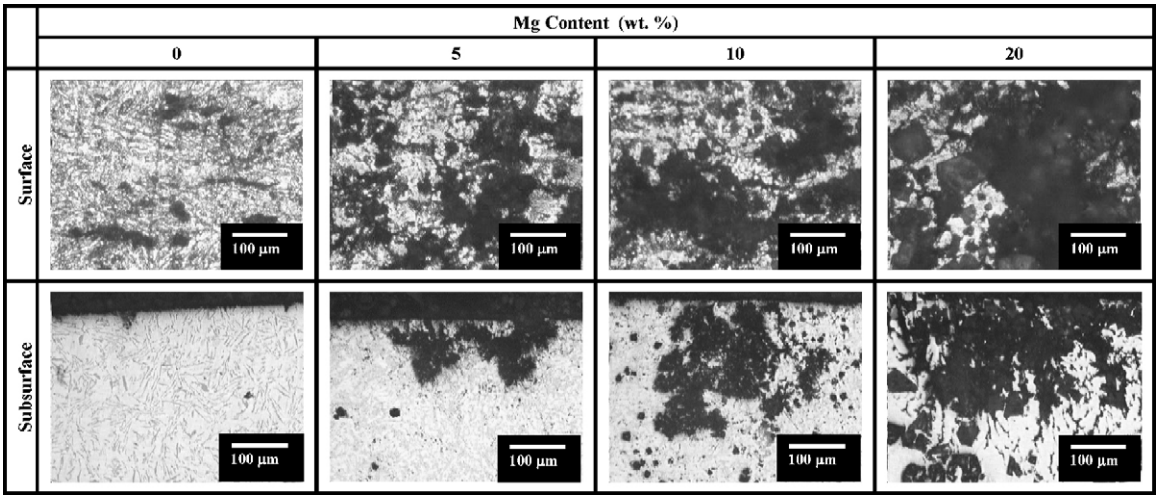

Fig. 7. LOM micrographs of the surfaces and cross-sections of the investigated alloys after corrosion tests.

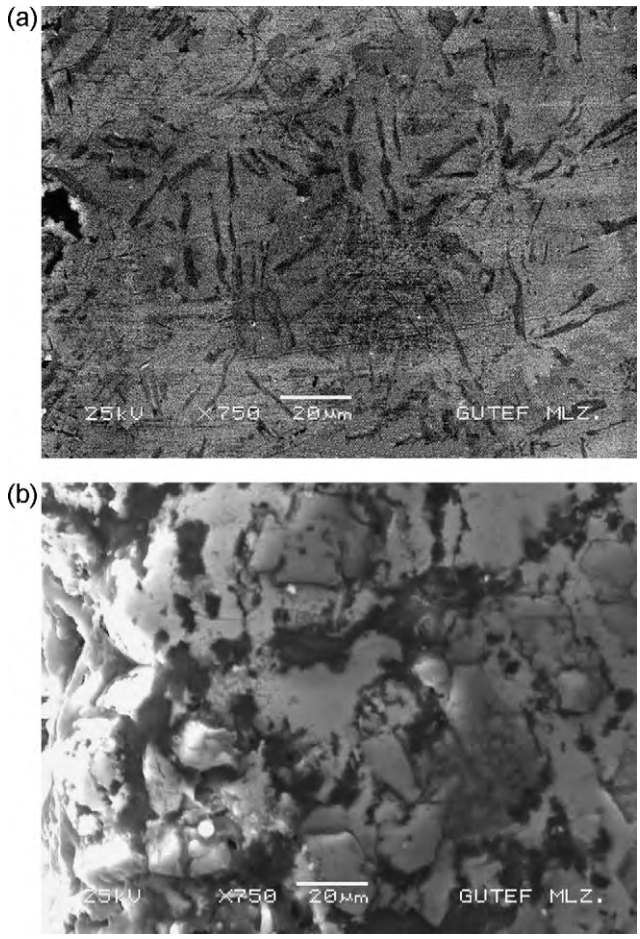

Fig. 8. SEM micrographs of the cross-sections of the corroded (a) Mg free and (b) 20 wt.% Mg containing alloys.

and propagated into the inner sections with increasing the Mg content, causing rougher surface appearance. SEM micrographs presented in Fig. 8a indicate that in the Mg free alloy the Al matrix adjacent to the Si needles was preferentially consumed by the corrosion. It is suggested that the Si needles effectively acted as a cathode and the Al matrix became anode in galvanic cell [30–32]. In the case of the Al–12Si–*X*Mg alloys, the corrosion loss can be correlated with the primary Mg_2Si particles, which remained in the microstructures of the corroded alloys (Fig. 8b). Since the Chinese script Mg_2Si phases and Si needles were refined on the Al–12Si–20Mg alloy microstructure (Fig. 1), it is suggested that the primary Mg_2Si particles acted as a cathode during the corrosion tests. Thus, the 20% Mg addition to the Al–12Si alloy resulted in the increase in the number of the weaker spots in the microstructure and the corrosion quickly progressed by the dissolution of the matrix as reported by Winkler and Flower [33]. Detrimental effect of intermetallics such as $MgZn_2$, Mg_2Si and Al_2CuMg on the corrosion resistance of Al alloys has also been reported in the literature. It is essential that alloying elements, to improve mechanical properties, should limit precipitation of intermetallics in the microstructure of Al alloys not to sacrifice the corrosion resistance [30–37].

4. Conclusions

The following conclusions can be drawn from the results of the present investigation conducted on the hot extruded Al–12Si–*X*Mg alloy, varying Mg content between 0 wt.% to 20 wt.%.

The microstructure of the Al–12Si–*X*Mg alloys consisted of the Si needles and Mg_2Si precipitates (as primary polygonal precipitates and as a component of Chinese script) in the Al matrix, while in the microstructure of the Mg free alloy the Mg_2Si type intermetallic precipitation was not detected. The volume fraction and size of the primary polygonal Mg_2Si particles increased with increasing the Mg content of the alloy. The Mg addition increased the hardness and compression strength of the Al–12Si–*X*Mg alloys attributed to the increase of the Mg_2Si precipitation. The corrosion loss of the Al–12Si–*X*Mg alloys in "30 g/l NaCl + 10 ml/l HCl" solution increased with increasing the Mg content and progressed by preferentially consumption of the Al matrix adjacent to the primary Mg_2Si particles.

Acknowledgements

This work was supported by the Research Fund of the Scientific and Technical Research Council of Turkey (TUBITAK) in the framework of the support programme for scientific and technological research projects concerning "Development of Alternative Composite Manufacturing Techniques For High Specific Strength Engineering Applications and Widening Its Usage In Turkey". I also express sincere appreciation to Prof. Dr. Huseyin CİMENOGLU from Istanbul Technical University for his valuable discussions and comments.

References

[1] M.A. Martinez, A. Martin, J. Llorca, Scripta Met. 28 (1993) 207–212.
[2] S.-W. Lai, D.D.L. Chung, J. Mater. Sci. 29 (1994) 3128–3150.
[3] H. Torabian, J.P. Patak, S.N. Tiwari, J. Mater. Sci. Lett. 14 (1995) 1631–1632.
[4] M. Suery, L. Lajoye, in: P. Rohatgi (Ed.), Solidification of Metal Matrix Composites, The Minerals Metals and Materials Society, 1990.
[5] H. Ahlatci, E. Candan, H. Cimenoglu, Metall. Mater. Trans. A 35 (2004) 2127–2141.
[6] E. Candan, H.V. Attkinson, H. Jones, Key Eng. Mater. 127 (1997) 463–470.
[7] I.A. Ibrahim, F.A. Mohammed, E.J. Lavernia, J. Mater. Sci. 26 (1991) 1137–1156.
[8] E.E. Schmid, K. von Oldenburg, G. Frommeyer, Z. Metallkd. 81 (1980) 809–815.
[9] G. Frommeyer, S. Beer, K. von Oldenburg, Z. Metallkd. 85 (1994) 372–376.
[10] Y.L. Liu, S.B. Kang, J. Mater. Sci. 32 (1997) 1443–1447.
[11] J. Zhang, Yu-Q. Wang, Ben-L. Zhou, Xing-Q. Wu, J. Mater. Sci. Lett. 17 (1998) 1677–1679.
[12] J. Kim Joong, D. Kim Hyang, K.S. Shin, J.N. Kim, Scripta Mater. 41 (1999) 333–340.
[13] J. Zhang, Z. Fan, Y. Wang, B. Zhou, Mater. Des. 21 (2000) 149–153.
[14] J. Zhang, Z. Fan, Y.Q. Wang, B.L. Zhou, Mater. Sci. Eng. A 281 (2000) 104–112.
[15] X.S.C. Tjong, Z.Y. Ma, Mater. Sci. Eng. R 29 (2000) 49–113.
[16] J. Zhang, Z. Fan, Y.Q. Wang, B.L. Zhou, J. Mater. Sci. Lett. 19 (2000) 1825–1828.
[17] L. Hengcheng, S. Yu, S. Guoxiong, Mater. Sci. Eng. A 358 (2003) 164–170.
[18] Y.G. Zhao, Q.D. Qin, Y.Q. Zhao, Y.H. Liang, Q.C. Jiang, Mater. Lett. 58 (2004) 2192–2194.
[19] M. Usta, M.E. Glicksman, R.N. Wright, Metall. Mater. Trans. 35 (A) (2004) 435–438.
[20] D.J. Chakrabarti, D.E. Laughlin, Prog. Mater. Sci. 49 (2004) 389–410.
[21] Y.G. Zhao, Q.D. Qin, Y.H. Liang, W. Zhou, Q.C. Jiang, J. Mater. Sci. 40 (2005) 1831–1833.
[22] Y.G. Zhao, Q.D. Qin, W. Zhou, Y.H. Liang, J. Alloys Compd. 39 (2005) 1–4.
[23] H.Y. Wang, Q.C. Jiang, B.X. Ma, Y. Wang, J.G. Wang, J.B. Li, J. Alloys Compd. 387 (2005) 105–108.
[24] W. Qudong, C. Yongjun, C. Wenzhou, W. Yinhong, Z. Chunquan, D. Wenjiang, Mater. Sci. Eng. A 394 (2005) 425–434.
[25] M. Zha, H.Y. Wang, P.F. Xue, L.L. Li, B. Liu, Q.C. Jiang, J. Alloys Compd. 472 (2009) 18–22.
[26] H.-Y. Wang, M. Zha, B. Liu, D.-M. Wang, Q.-C. Jiang, J. Alloys Compd. 480 (2009) 25–28.
[27] C. Li, Y. Wu, H. Li, X. Liu, J. Alloys Compd. 477 (2009) 212–216.
[28] K. Chen, Z.Q. Li, J.S. Liu, J.N. Yang, Y.D. Sun, S.G. Bian, J. Alloys Compd. 487 (2009) 293–297.
[29] E. Nembach, Particle Strengthening of Metals and Alloys, John Wiley, New York, 1997.
[30] J.R. Scully, D.E. Peebles, A.D. Romig, D.R. Frear, Metall. Trans. 23 A (1992) 2641–2655.
[31] Z. Szklarska-Smialowska, Corros. Sci. 41 (1999) 1743–1767.
[32] N. Birbilis, R.G. Buchheit, J. Electrochem. Soc. 152 (2005) 140–151.
[33] S.L. Winkler, H.M. Flower, Corros. Sci. 46 (2004) 903–915.
[34] G.S. Frankel, J. Electrochem. Soc. 145 (1998) 2186–2198.
[35] W. Zhang, G.S. Frankel, J. Electrochem. Soc. 149 (2002) 510–519.
[36] S.S. Abde Rahim, H.H. Hassan, M.A. Amin, Corros. Sci. 46 (2004) 1921–1938.
[37] T.-S. Huang, G.S. Frankel, Corros. Eng. Sci. Technol. 41 (2006) 192–199.